Environmental Science and Ecotechnology 9 (2022) 100146

Contents lists available at ScienceDirect

Environmental Science and Ecotechnology

journal homepage: www.journals.elsevier.com/environmental-science-and-ecotechnology/

Original Research

Sustainable treatment of nitrate-containing wastewater by an autotrophic hydrogen-oxidizing bacterium

Yi-Zhen Chen [a], Li-Juan Zhang [a, **], Ling-Yun Ding [a, b], Yao-Yu Zhang [a], Xi-Song Wang [a], Xue-Jiao Qiao [a], Bao-Zhu Pan [c], Zhi-Wu Wang [d], Nan Xu [a], Hu-Chun Tao [a, *]

[a] Key Laboratory for Heavy Metal Pollution Control and Reutilization, School of Environment and Energy, Peking University Shenzhen Graduate School, Shenzhen, 518055, Guangdong, China
[b] College of Health Science and Environmental Engineering, Shenzhen Technology University, Shenzhen, 518118, Guangdong, China
[c] State Key Laboratory of Eco-hydraulic in Northwest Arid Region of China, Xi'an University of Technology, Xi'an, 710048, Shaanxi, China
[d] Department of Civil and Environmental Engineering, Virginia Polytechnic Institute and State University, Manassas, 20147, Virginia, USA

ARTICLE INFO

Article history:
Received 9 November 2021
Received in revised form
19 January 2022
Accepted 20 January 2022

Keywords:
Wastewater
Nitrate
Hydrogen-oxidizing bacteria
Autotrophic assimilation
Aerobic denitrification

ABSTRACT

Bacteria are key denitrifiers in the reduction of nitrate (NO_3^--N), which is a contaminant in wastewater treatment plants (WWTPs). They can also produce carbon dioxide (CO_2) and nitrous oxide (N_2O). In this study, the autotrophic hydrogen-oxidizing bacterium *Rhodoblastus* sp. TH20 was isolated for sustainable treatment of NO_3^--N in wastewater. Efficient removal of NO_3^--N and recovery of biomass nitrogen were achieved. Up to 99% of NO_3^--N was removed without accumulation of nitrite and N_2O, consuming CO_2 of 3.25 mol for each mole of NO_3^--N removed. The overall removal rate of NO_3^--N reached 1.1 mg L^{-1} h^{-1} with a biomass content of approximately 0.71 g L^{-1} within 72 h. TH20 participated in NO_3^--N assimilation and aerobic denitrification. Results from ^{15}N-labeled-nitrate test indicated that removed NO_3^--N was assimilated into organic nitrogen, showing an assimilation efficiency of 58%. Seventeen amino acids were detected, accounting for 43% of the biomass. Nitrogen loss through aerobic denitrification was only approximately 42% of total nitrogen. This study suggests that TH20 can be applied in WWTP facilities for water purification and production of valuable biomass to mitigate CO_2 and N_2O emissions.

1. Introduction

Greenhouse gas (GHG) emissions from wastewater treatment plants (WWTPs) have attracted increasing attention worldwide. Biological processes play a key role in treatment of wastewater containing oxidized contaminants such as nitrate (NO_3^--N). Heterotrophic denitrification bacteria in these processes release considerable amounts of carbon dioxide (CO_2) [1]. In an incomplete denitrification process, denitrification bacteria can also produce nitrous oxide (N_2O) and dinitrogen (N_2) [2]. The global warming potential of N_2O is 273 times that of CO_2 on a 100-year timescale [3]. It has been estimated that the level of reactive nitrogen pollution influencing the climate in 2050 will be up to 56% higher than that in 2010 [4]. This increase will boost demand for sustainable techniques to treat NO_3^--N in WWTPs.

Certain denitrifiers such as *Pseudomonas stutzeri* TR2 [5], *Vibrio* sp. Y1-5 [6], *Marinobacter* strain NNA5 [7], and *Pseudomonas mendocina* LYX [8] could feasibly reduce N_2O emissions. However, these heterotrophic strains also produce CO_2 from organic electron donors during NO_3^--N removal from wastewater. Autotrophic bacteria are promising candidates to mitigate GHG emissions from NO_3^--N treatment without the need for added organic compounds [9,10]. They are very attractive for use in WWTPs in terms of nutrient recovery via nitrogen assimilation. Recently, hydrogen-oxidizing bacteria (HOB) have been proposed to improve the sustainability of wastewater treatment through assimilation of nitrogen via rapid autotrophic growth on CO_2 as a carbon source and hydrogen (H_2) as an energy source [11]. HOB can develop niche adaptations to oxic–anoxic environments [12], which can shed light on the feasibility of GHG mitigation in WWTPs where dissolved oxygen (DO) and NO_3^--N concentrations fluctuate. On one hand, autotrophic HOB obtain electrons from H_2, and can quickly

* Corresponding author.
** Corresponding author.
E-mail addresses: zhanglj@pkusz.edu.cn (L.-J. Zhang), taohc@pkusz.edu.cn (H.-C. Tao).

https://doi.org/10.1016/j.ese.2022.100146

generate energy and spontaneously capture CO_2 released by heterotrophic bacteria in wastewater or sludge [13]. On the other hand, inorganic nitrogen is simultaneously assimilated into biomass nitrogen, such as cellular proteins consisting of amino acids [14]. NO_3^--N removal by HOB does not release CO_2 or N_2O, and value-added products such as single-cell proteins and biopolymers are recovered from removed NO_3^--N [15]. To date, most studies have been carried out using mixed HOB cultures for biomass production [16–18], which makes it difficult to explore complex pathways of nitrogen metabolism. Therefore, novel HOB strains and their specific pathways of nitrogen utilization are highly desirable for sustainable treatment of nitrate-containing wastewater.

In this study, a newly isolated HOB strain, *Rhodoblastus* sp. TH20, was evaluated for NO_3^--N removal from wastewater. The pathways of NO_3^--N reduction were investigated in the presence of O_2. TH20 grew rapidly on CO_2 and efficiently removed NO_3^--N under the optimum conditions. NO_3^--N was consumed as the predominant electron acceptor without inhibition under an aerobic atmosphere. ^{15}N-labeled-nitrate test, 16S rRNA gene sequencing, and genome-wide scanning were conducted to verify the nitrogen metabolism pathways. Autotrophic TH20 is a potential candidate to develop sustainable methods for mitigation of GHG emissions, reduction of nitrogen loss, and reclamation of clean water in WWTPs.

2. Materials and methods

2.1. Strain isolation and cell culture

TH20 (GenBank No. MK968713.1) was isolated from activated sludge in a WWTP in Guangdong, China (Text S1). The isolated strains (TH20 cells with a volume ratio of 5% and an optical density at 600 nm of 1.20) were cultured in 70 mL of mineral medium in a 250-mL airtight serum bottle. The mineral medium (1.0 L) contained KNO_3 (0.58 g), KH_2PO_4 (0.5 g), $NaHCO_3$ (0.5 g), $MgSO_4 \cdot 7H_2O$ (0.2 g), $CaCl_2$ (0.003 g), $(NH_4)_2Fe(SO_4)_2 \cdot 6H_2O$ (0.02 g), and trace element solution (0.5 mL). The trace element solution (1.0 L, pH 7.0) contained $CoCl_2 \cdot 6H_2O$ (0.119 g), $NiCl_2 \cdot 6H_2O$ (0.118 g), and $CuSO_4 \cdot 5H_2O$ (0.156 g). The mineral medium was sterilized at 121 °C for 20 min, and was cooled to room temperature before use. The $(NH_4)_2Fe(SO_4)_2 \cdot 6H_2O$ solution was sterilized by filtration through a 0.22-μm membrane filter, and was injected into the mineral medium separately. The bottle was purged with a mixture of H_2, O_2, and CO_2 (70:20:10, v/v) gases [19], and then placed in a rotary shaker for agitation.

2.2. Experimental design

Nitrogen removal by TH20 was tested under different operating parameters with NO_3^--N as the nitrogen source. We tested five different pH values (5.0, 6.0, 7.0, 8.0, and 9.0; adjusted using 6 M NaOH and/or 6 M HCl), temperatures (20 °C, 25 °C, 30 °C, 35 °C, and 40 °C), agitation speeds (80, 120, 160, 200, and 240 rpm), and initial NO_3^--N concentrations (0, 20, 50, 80, and 100 mg L^{-1}; adjusted by adding KNO_3 to the mineral medium). When NO_3^--N and NO_3^--N + NH_4^+-N were added as nitrogen sources, the fate of nitrogen was determined under the optimum parameters. The concentrations of different nitrogen species (NO_3^--N, NO_2^--N, NH_4^+-N, and total nitrogen) were measured. Gas mixtures were tested every 24 h, i.e., at 0, 24, 48, and 72 h, headspace gas (10 mL) was collected to determine H_2, O_2, and CO_2 consumption and NO, N_2O, and N_2 production. Meanwhile, the exhausted headspace gas was replaced with a mixture of H_2, O_2, and CO_2 (70:20:10, v/v). All experiments were performed in triplicate unless otherwise specified.

A ^{15}N-labeled-nitrate test was carried out to investigate nitrogen transformation during NO_3^--N removal by TH20. The NO_3^--N in the culture medium was replaced with $^{15}NO_3^-$-N (15% amount-of-substance fraction; Shanghai Research Institute of Chemical Industry, Shanghai, China) at an initial concentration of 80 mg L^{-1}. The test was conducted at pH 7.0 and 25 °C with an agitation speed of 200 rpm. After incubation for 36 h, samples were taken for analyses of $^{15}NO_3^-$-N, $^{15}NO_2^-$-N, $^{15}NH_4^+$-N, $^{15}N_{org\text{-}N}$, ^{15}NO, $^{15}N_2O$, and $^{15}N_2$.

16S rRNA gene sequencing and genome-wide scanning were conducted to clarify the specific genes in TH20. Bacterial cells were collected for genome-wide scanning data evaluation and quality control, genome splicing and assembly, and gene prediction and gene annotation. The gene functionalities and pathway maps were derived from the Kyoto Encyclopedia of Genes and Genomes database [20]

2.3. Measurement and analysis

A spectrophotometer (DR6000, Hach, Loveland, CO) was used to determine the NO_3^--N, NO_2^--N, NH_4^+-N, and total nitrogen concentrations [21] and cell optical density at 600 nm. The specific growth rates for TH20 were calculated using the Monod equation: $S/\mu = S/\mu_{max} + K_s/\mu_{max}$, where S is the concentration of the rate-limiting substrate (mg L^{-1}), μ is the specific growth rate (h^{-1}), μ_{max} is the maximum specific growth rate (h^{-1}), and K_s is the concentration giving one-half the maximum rate (mg L^{-1}) [22]. The dry cell weight (DCW) was determined by centrifugation of the biomass at 4 °C and 10,000 rpm for 3 min, followed by evaporation at 105 °C for 2 h [23]. Dissolved gases were purged from the culture medium with helium gas at 40 mL min^{-1} for 10 min. Headspace gases (10 mL) were determined using a gas chromatograph (7890B, Agilent, Santa Clara, CA) equipped with a thermal conductivity detector for O_2, CO_2, NO, N_2O, and N_2, and a flame ionization detector for H_2 [24,25]. Stable ^{15}N isotopes were analyzed by chemical conversion and combustion methods using an isotope analyzer (IsoPrime100, Elementar, Langenselbold, Germany). The functional groups in the biomass components were characterized by Fourier transform infrared spectrometry (Spectrum 100, PerkinElmer, Waltham, MA). A CHNS/O elemental analyzer (Vario EL cube, Elementar, Germany) was used to analyze the elemental composition of the biomass. The expression levels of genes related to nitrogen metabolism with different nitrogen sources were investigated by real-time quantitative polymerase chain reaction (qRT-PCR). Genomic RNA was extracted using a Sangon Bacterial RNA Kit (B511321, Sangon Biotech, Shanghai, China), and cDNA synthesis was performed. According to the gene sequences derived from genome-wide scanning, PCR primers were designed using Premier 5.0 software (PREMIER Biosoft, San Francisco, CA). Amplification was performed with a thermal cycler (TC-XP-G, Bioer Technology, Hangzhou, China). PCR was conducted on a 25-μL sample with initial denaturation at 95 °C for 3 min, followed by 35 cycles of 30 s at 95 °C, 30 s at 57 °C, and 30 s at 72 °C, and then a final extension at 72 °C for 8 min. All quantitative amplifications were performed in triplicate on a StepOne PCR instrument (Thermo Fisher Scientific, Waltham, MA) with a SYBR Green qRT-PCR Kit (B639271, Sangon Biotech, Shanghai, China) and the relevant primers. All trials were performed in parallel ($n = 6$). The activity of nitrous oxide reductase (N_2OR) was measured by an enzyme-linked immunosorbent assay following the kit instruction manual (JK142666, Enzyme Linked Biotechnology, Shanghai, China).

3. Results and discussion

3.1. Nitrate removal by autotrophic TH20

TH20 was able to consume NO_3^--N for autotrophic growth under aerobic conditions. The efficacy of TH20 in NO_3^--N removal was

affected by the temperature, pH, agitation speed, and initial NO_3^--N concentration.

Generally, most microorganisms that can remove NO_3^--N are sensitive to the culture temperature because it can affect the function of all enzymes involved in the auto-hydrogenotrophic NO_3^--N removal process [26]. TH20 grew most rapidly at 25 °C (Fig. 1a), reaching a μ_{max} of 0.10 h^{-1} in the early logarithmic period (24–36 h). The time needed to achieve rapid cell propagation decreased at higher temperature. At 25–35 °C, TH20 had a relatively short adaptive period and then entered a logarithmic growth period after 12 h. However, TH20 entered a decay period after 36 h at 35 °C possibly because of the formation of a large amount of NO_2^--N (27.35 ± 0.61 mg L^{-1}, Table S1). There was consequently a sharp decrease in the NO_3^--N concentration from 24 h to 36 h. Cell growth of TH20 was inhibited by accumulation of NO_2^--N, which suggested that the impact of changes in the temperature on nitrite reductase was more notable than that of NO_3^--N reductase. Cell growth of TH20 was markedly inhibited at 40 °C. The μ_{max} decreased to 0.06 h^{-1} at 12 h under this condition, and then TH20 entered a decay period. From 24 h onwards, the NO_2^--N concentration increased from 18.63 ± 0.20 mg L^{-1} to its highest concentration (28.04 ± 0.08 mg L^{-1}) at 72 h. At 25 °C, the overall NO_3^--N removal rate was approximately 1.1 mg L^{-1} h^{-1}. More than 99% of NO_3^--N was removed throughout the testing period. Therefore, 25 °C was the optimum temperature for TH20 growth.

Cell growth of TH20 was slightly affected by pH in the tested range (5.0–9.0). The μ_{max} changed slightly (Fig. 1b); however, TH20 cells grew better under neutral and weakly alkaline conditions than under stronger alkaline and acidic conditions. The dominant species in solution under neutral and weakly alkaline conditions was HCO_3^- (Fig. S1), contributing more significantly as carbon source to support the growth of TH20. Similar results have been reported for hydrogenotrophic denitrifying bacteria, which grew faster when HCO_3^- was used as the sole carbon source [27]. When the pH was lower than 7.0 or higher than 8.0, cell growth of TH20 decreased. The NO_3^--N removal from aqueous solution was strongly related to the pH value. The lowest NO_3^--N removal rate (0.90 mg L^{-1} h^{-1}) was obtained at pH 5.0. The removal efficiency at this pH value was 83%. Expression of the *nirS* and *cnorB* genes in *Pseudomonas mandelii* also greatly decreased at pH 5.0; thus, removal of NO_3^--N was inhibited [28]. Therefore, expression of key enzymes in NO_3^--N removal by TH20 and related functional genes was proposed to also be affected by pH. In order to achieve higher NO_3^--N removal accompanied by considerable cell growth, the pH value was optimized at 7.0.

The agitation speed affected gas dissolution and transfer into or release from the aqueous phase [29]. Dissolved H_2 and DO simultaneously affected the growth of TH20. The solubility of H_2 is low (1.6 mg L^{-1} at 20 °C) and the concentration of dissolved H_2 in the bulk solution is very dependent on the agitation speed. The best cell growth and NO_3^--N removal with TH20 were obtained at an agitation speed of 200 rpm (Fig. 1c). When the speed was decreased to 80 rpm, only 55% of NO_3^--N was removed within 72 h. The μ_{max} occurred at 48 h, which was later than under other agitation speeds. With this agitation speed, TH20 did not have enough dissolved H_2 as energy to grow. Accumulation of NO_2^--N occurred with a maximum concentration of 13.81 ± 0.03 mg L^{-1} at 36 h (data not shown). At 200 rpm, the amount of dissolved H_2 could meet the requirements for cell growth, which was not inhibited by DO. When the agitation speed was lower than 200 rpm, the μ_{max} was elevated by higher contents of dissolved H_2. The decreased cell growth of TH20 at 240 rpm may be caused by inhibition with a high concentration of DO. A DO threshold for aerobic NO_3^--N removal has been proposed and indicated that the conversion rates of NO_3^--N and DO can be controlled through three routes (Fig. S2). Most aerobic microorganisms consume NO_3^--N through route II, some through route III, and a few through route I [30]. The NO_3^--N consumption by TH20 increased from the agitation speed of 80 rpm–200 rpm, and then decreased at 240 rpm, which was likely to follow pathway II.

The effects of the initial NO_3^--N concentration on TH20 growth and NO_3^--N removal were investigated (Fig. 1d). The optimum NO_3^--N concentration for TH20 growth was 80 mg L^{-1}, and vigorous growth occurred under this condition. For all concentrations, TH20 was in an adaptation period for the first 12 h, and the growth patterns did not differ much. After entering a logarithmic phase at low NO_3^--N concentrations that were not sufficient for the growth of TH20, the growth patterns began to show differences. Hence a sufficient supply of nitrogen is crucial to cell propagation. With an initial NO_3^--N concentration of 80 mg L^{-1}, the removal efficiency peaked at approximately 99% and the removal rate was 1.55 mg NO_3^--N per g DCW per h. This NO_3^--N removal capability of TH20 was higher than those reported for heterotrophic denitrifiers with and without continuous glucose feed in membrane bioreactors (1.20 and 0.40 mg NO_3^--N per g DCW per h) [31]. Another study that had similar results to ours showed that the removal rate increased

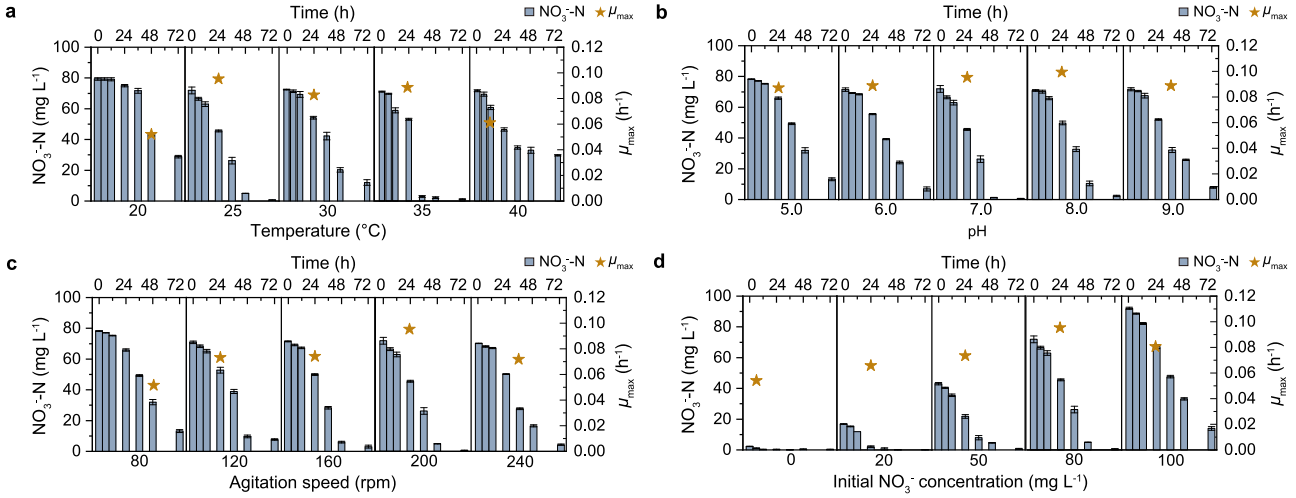

Fig. 1. The effects of (a) temperature, (b) pH, (c) agitation speed, and (d) initial nitrate concentration on the efficacy of nitrate removal and autotrophic growth of TH20 cells.

with NO_3^--N availability in bulk solutions [32]. The first-order kinetics fitted the NO_3^--N removal data well in two stages (Fig. S3). Slow NO_3^--N removal with a lower rate constant (0.03 h^{-1}) occurred in the adaptive growth period of TH20, and rapid NO_3^--N removal with a higher rate constant (0.09 h^{-1}) occurred between 24 and 72 h when the μ_{max} was obtained for TH20 growth. The NO_3^--N removal kinetics agreed with the Monod parameters, indicating a high correlation between NO_3^--N removal and TH20 growth.

3.2. The fate of nitrate nitrogen used by TH20

Transformation of nitrogen was explored under the optimum growth conditions of TH20 with 80 mg L^{-1} NO_3^--N as the nitrogen source (Fig. 2a). The NO_3^--N concentration decreased greatly from 80 mg L^{-1} to less than 1 mg L^{-1} after 72 h. This gave a NO_3^--N removal efficiency of >99%, which was greater than that by *Pseudomonas putida* Y-9 (82%) under aerobic conditions [33]. In contrast to other aerobic denitrifiers, such as *Pseudomonas stutzeri* PCN-1 [34], *Paracoccus versutus* LYM [35], *Pseudomonas* sp. ADN-42 [36], and *Marinobacter* sp. NNA5 [7] that primarily converted NO_3^--N into N_2, TH20 assimilated NO_3^--N to biomass nitrogen (58%) with accompanying aerobic denitrification to N_2 (42%). This contributed to mitigation of nitrogen loss from the biosphere to atmosphere in nitrate-containing wastewater treatment. The transformation rate of NO_3^--N to N_2 was markedly higher in the first 24 h. From 36 h onwards, more NO_3^--N was converted to biomass nitrogen. It was noted that approximately 4 mg L^{-1} NH_4^+-N was detected during NO_3^--N reduction between 12 and 24 h, and this then decreased steadily from 24 to 72 h. As a ubiquitous contaminant in wastewater, NH_4^+-N was more favorable than NO_3^--N for assimilation into biomass nitrogen by TH20 (Fig. 2b). When NO_3^--N (40 mg L^{-1}) and NH_4^+-N (40 mg L^{-1}) were used as the nitrogen sources, the overall efficiency of aerobic denitrification decreased to 22% and more nitrogen was assimilated into biomass nitrogen (78%) than when NO_3^--N (80 mg L^{-1}) was used as the nitrogen source. Bacterial cell synthesis competed with aerobic denitrification of NO_3^--N to N_2 for electrons and energy in the presence of NH_4^+-N. Neither NO_2^--N nor N_2O was observed during the transformation of NO_3^--N and NH_4^+-N by TH20 under the optimum conditions. Hence NO_3^--N was efficiently assimilated into biomass along with CO_2, which reduced GHG emissions from WWTPs.

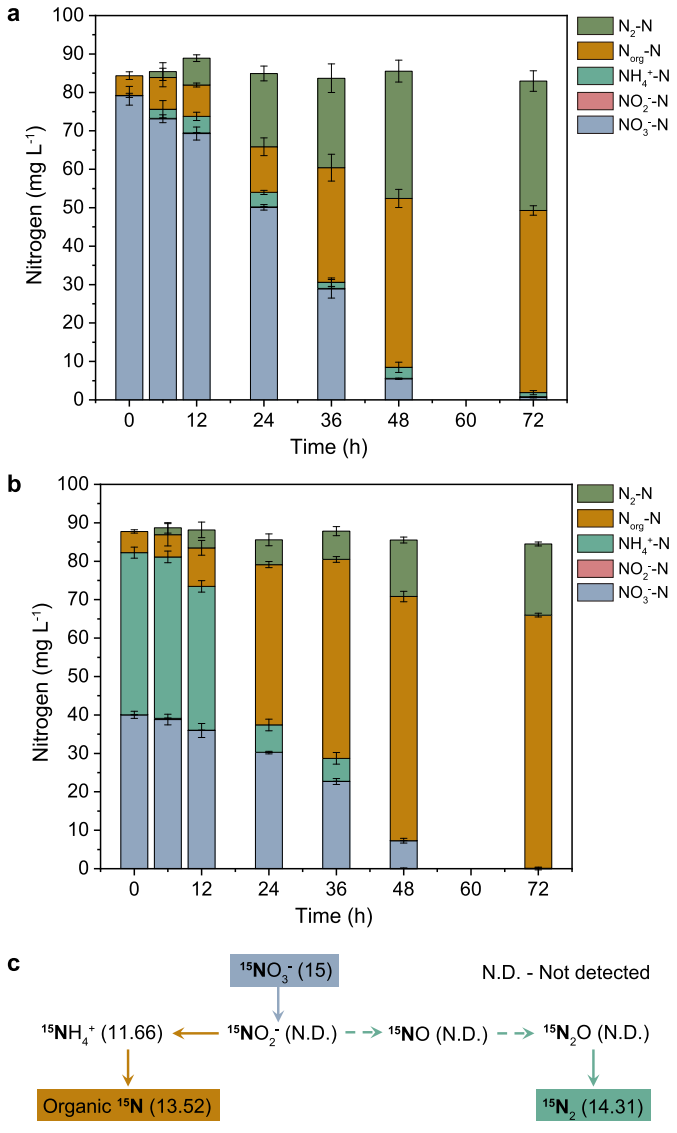

Fig. 2. The transformation of nitrogen by TH20 with (a) 80 mg L^{-1} NO_3^--N, (b) 40 mg L^{-1} NO_3^--N and 40 mg L^{-1} NH_4^+-N, and (c) 80 mg L^{-1} $^{15}NO_3^-$-N (abundance % at 36 h) as the nitrogen sources under the optimum conditions.

The results of ^{15}N-labeled-nitrate test are shown in Fig. 2c. After 36 h of growth in the $^{15}NO_3^-$-containing medium, $^{15}NH_4^+$-N was detected at 1.62 mg L^{-1} and the ^{15}N isotope ratio was 11.66%. This confirmed that the dissimilatory nitrate reduction to ammonium (DNRA) pathway was associated with production of organic nitrogen. In addition, the biomass nitrogen content was 29.80 mg L^{-1}, with a ^{15}N abundance of 13.52%. Therefore, autotrophic assimilation (NO_3^--N → NH_4^+-N → biomass nitrogen) was further involved after DNRA, and the assimilation efficiency of autotrophic TH20 (58%–78%) was notably higher than that of heterotrophic *Pseudomonas stutzeri* T13 (47%) [37]. These results indicated that TH20 could effectively reduce nitrogen and carbon loss to secure the resources in nitrate-containing wastewater.

3.3. Mechanism of nitrate removal by TH20

Aerobic denitrification, DNRA, and ammonium assimilation (glutamine synthetase, EC 6.3.1.2; glutamate synthase, EC 1.4.1.13; and glutamate dehydrogenase, EC 1.4.1.3) co-occurred during nitrogen removal by TH20 with 80 mg L^{-1} NO_3^--N as the nitrogen source (Figs. 3a and S4). In addition, the nitrogen fixation pathway occurred with evidence of *nifDKH* genes detected. Similar pathways of nitrogen metabolism but higher levels of assimilation gene expression were detected for TH20 with 40 mg L^{-1} NO_3^--N and 40 mg L^{-1} NH_4^+-N as the nitrogen sources (Fig. S5). This indicated there were flexible metabolism modes for TH20 grown on different nitrogen sources.

Twelve genes involved in nitrogen metabolism by TH20 were quantitatively determined by qRT-PCR under the optimum growth conditions (Fig. 3b). In the denitrification pathway, higher expression of genes *nirS* and *nirK* (1.32 and 1.37 × 10^6 copies per μg RNA) for NO_2^--N reduction than of genes *narI*, *narH*, and *narG* (4.21, 5.66, and 8.05 × 10^5 copies per μg RNA) for NO_3^--N reduction demonstrated that NO_2^--N reduction was faster than NO_3^--N reduction. The enzyme reactivity of N_2OR (encoded by gene *nosZ*) further explained the negligible amount of N_2O produced in aerobic denitrification. The N_2OR activities at 24–36 h were 2–4 times of those at 48–72 h (Fig. 3c), which showed that conversion of N_2O to N_2 catalyzed by N_2OR was highly efficient in rapid TH20 growth periods. These results explained the minimal accumulation of NO_2^--N and N_2O during NO_3^--N removal by TH20 via aerobic denitrification. In the NO_3^--N assimilation pathway, the abundance of *nirB* in TH20 was higher than that of *nasA*, indicating that transformation

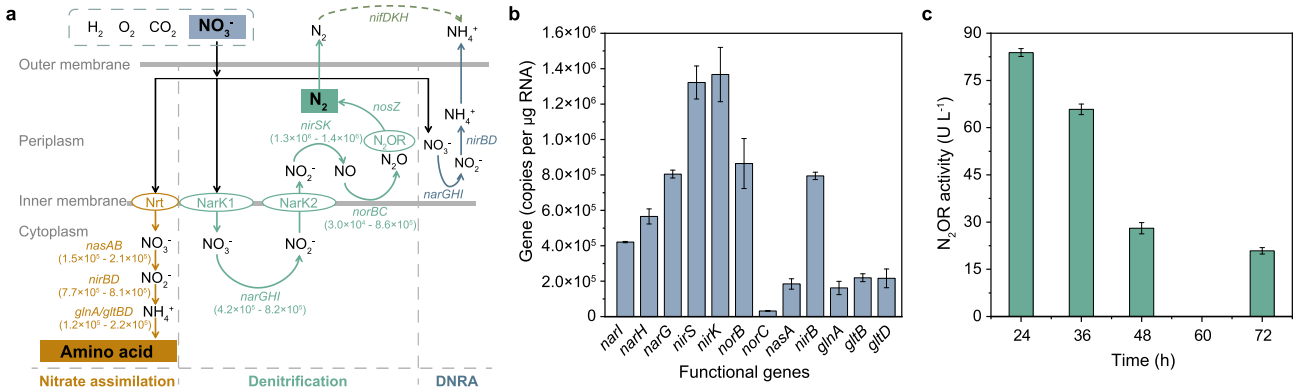

Fig. 3. (a) Nitrogen metabolism pathways with gene abundance (copies per μg RNA), (b) quantification of respective functional genes, and (c) enzyme activity of nitrous oxide reductase (N_2OR) in TH20 under the optimum conditions.

of NO_3^--N → NO_2^--N → NH_4^+-N occurred. The lower expression of genes *glnA*, *gltB*, and *gltD* suggested that the formed NH_4^+-N was partly converted into amino acids.

3.4. Amino acid production by TH20

Changes in the amino acid profile were used to verify the conversion of NO_3^--N into amino acids (Fig. 4). The DCW of TH20 was 0.71 g L^{-1}, and 43% of this was composed of seventeen amino acids, including eight essential amino acids. Glutamic acid, aspartic acid, alanine, and leucine were the four most abundant amino acids, with contents higher than 3 g per 100 g DCW. Glutamic acid and aspartic acid are raw materials for the synthesis of nucleotides [38,39], and the high contents of these amino acids in TH20 will facilitate the formation of nucleotides. Leucine is the most effective branched-chain amino acid, and is often involved in protein synthesis and energy metabolism [40,41]. The Fourier transform infrared results (Fig. S6) further demonstrated that NO_3^--N was transformed into organic nitrogen and stored intracellularly. The elemental composition (Table S2) gave a molecular formula for TH20 cells of $C_{5.60}H_{12.69}O_{3.52}N$. The nitrogen content of TH20 cells (9.32%) was close to that of the two most abundant amino acids, and higher than that of the autotrophic HOB *Paracoccus versutus* D6 (8.10%) [23]. Because TH20 primarily assimilated NO_3^--N into biomass nitrogen via autotrophic assimilation, CO_2 was simultaneously fixed into TH20 cells. The content of organic carbon was 44.74%, which was equal to the median content of seventeen amino acids. Therefore, rapid propagation of TH20 cells was evidenced by the changing profile of amino acids. Previous studies have demonstrated that HOB with NO_3^--N assimilation capability can be applied as biofertilizers [38]; therefore, TH20 could be used as a biofertilizer after NO_3^--N recovery.

3.5. Carbon sequestration by TH20

TH20 could grow autotrophically on CO_2 and efficiently sequestrate inorganic carbon into the cell biomass. No organic carbon was required, and no CO_2 was released. The molar ratios of CO_2 uptake against H_2 uptake ranged from 0.18 to 0.26 (Fig. 5). These values were consistent with the metabolic parameters for the growth of typical HOB [19]. In the logarithmic growth period, the highest CO_2/H_2 value was obtained for autotrophic TH20 cells, and the ratio agreed with the stoichiometry of carbon and energy utilization in Table 1. For each mole of NO_3^--N removed, 3.25 mol of CO_2 was consumed. The CO_2 fixed by TH20 was approximately 3 mol more than that fixed by mixed autotrophic strains in activated sludge and biofilms [42,43]. By contrast, oxidation of CH_3OH and CH_3CH_2OH as organic carbon sources during removal of 1 mol

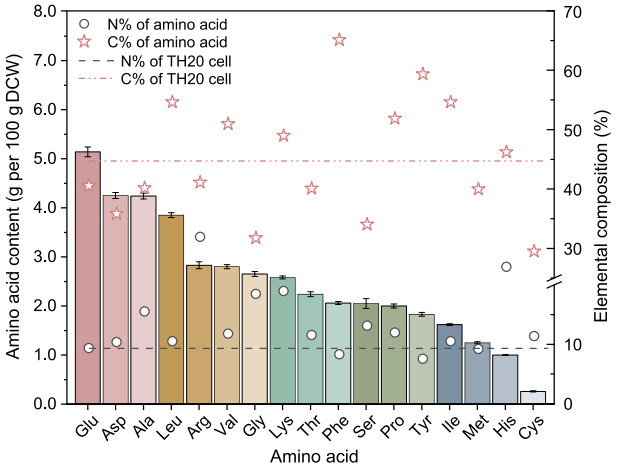

Fig. 4. Amino acid, nitrogen, and carbon contents of the bacterial biomass produced by TH20 under the optimum conditions.

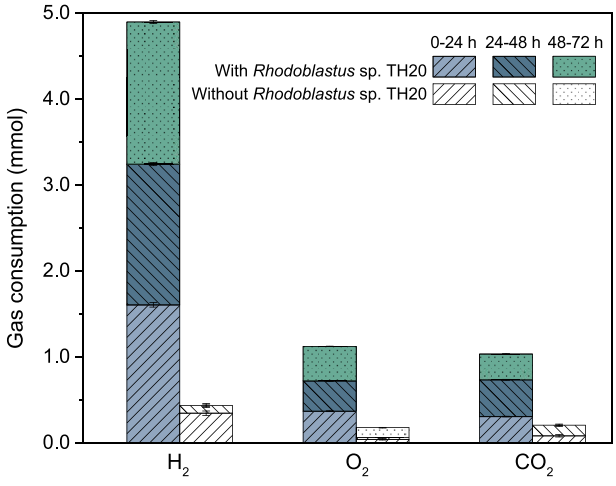

Fig. 5. Consumption of H_2, O_2, and CO_2 gas mixture by TH20 under the optimum conditions.

Table 1
CO_2 emission during nitrate removal by autotrophic and heterotrophic bacteria grown on different carbon sources.

Strain	Carbon source	Reaction	CO_2 emission (mol per mol nitrate)	Reference
Rhodoblastus sp. TH20	CO_2	$NO_3^- + 10.64\ H_2 + H^+ + 3.25\ CO_2 \rightarrow 0.58\ C_{5.60}H_{12.69}O_{3.52}N + 0.21\ N_2 + 7.46\ H_2O$	−3.25	This study
Activated sludge	CO_2	$NO_3^- + 2.82\ H_2 + H^+ + 0.14\ CO_2 \rightarrow 0.028\ C_5H_7O_2N + 0.49\ N_2 + 3.22\ H_2O$	−0.14	[42]
Biofilm	CO_2	$NO_3^- + 3.35\ H_2 + H^+ + 0.37\ CO_2 \rightarrow 0.074\ C_5H_7O_2N + 0.46\ N_2 + 3.59\ H_2O$	−0.37	[43]
Activated sludge	CH_3OH	$NO_3^- + H^+ + 1.08\ CH_3OH \rightarrow 0.065\ C_5H_7O_2N + 0.47\ N_2 + 0.76\ CO_2 + 2.44\ H_2O$	0.76	[44]
Biofilm	CH_3CH_2OH	$NO_3^- + H^+ + 0.67\ CH_3CH_2OH \rightarrow 0.13\ C_5H_7O_2N + 0.43\ N_2 + 0.68\ CO_2 + 2.04\ H_2O$	0.68	[22]

of NO_3^--N generated 0.76 mol of CO_2 in activated sludge processes and 0.68 mol of CO_2 in biofilm processes [22,44]. Net consumption of approximately 4 mol of CO_2 was achieved using autotrophic TH20 instead of heterotrophic denitrifying bacteria. In addition, TH20 grew faster for CO_2 sequestration and NO_3^--N assimilation into biomass under aerobic conditions than under anaerobic conditions (Fig. S7). This was possibly because of the large quantities of energy released from the hydrogen oxidation process [45]. In practical application, gaseous substrates of H_2 and O_2 (together with CO_2) need to be produced by green techniques such as microbial electrolysis cells with smaller power supplies [46]. Explosive H_2 and O_2 should always be treated with the utmost caution. With the implementation of green and safe processes, it will be possible to exploit TH20 for mitigation of GHG emissions in sustainable WWTPs.

4. Conclusions

The newly isolated HOB strain, *Rhodoblastus* sp. TH20, effectively removed 99% of NO_3^--N with an overall removal rate of approximately 1.1 mg L^{-1} h^{-1}. Autotrophic assimilation, aerobic denitrification, and DNRA pathways co-occurred with TH20. The NO_3^--N was primarily removed by autotrophic assimilation with synthesis of valuable amino acids and consumption of CO_2. No accumulation of NO_2^--N and N_2O occurred in the aerobic denitrification pathway. TH20 exhibited both efficient NO_3^--N removal and rapid recovery of biomass nitrogen. The excellent potential of autotrophic TH20 makes it a promising candidate to mitigate CO_2 and N_2O emissions in sustainable treatment of nitrate-containing wastewater.

Declaration of competing interest

The authors declare that they have no known competing financial interests or personal relationships that could have appeared to influence the work reported in this paper.

Acknowledgements

This work was funded by the Shenzhen Fundamental Research Programs (JCYJ20180503182122539, JCYJ20180503182130795, and GXWD20201231165807007-20200810165349001) and the National Natural Science Foundation of China (51939009). We appreciate the suggestions and help of Dr. Wei-Min Wu from Stanford University during manuscript preparation.

Appendix A. Supplementary data

Supplementary data to this article can be found online at https://doi.org/10.1016/j.ese.2022.100146.

References

[1] H.Y. Zheng, Y. Liu, X.Y. Gao, G.M. Ai, L.L. Miao, Z.P. Liu, Characterization of a marine origin aerobic nitrifying-denitrifying bacterium, J. Biosci. Bioeng. 114 (1) (2012) 33–37.
[2] G. Weigelhofer, T. Hein, Efficiency and detrimental side effects of denitrifying bioreactors for nitrate reduction in drainage water, Environ. Sci. Pollut. Res. 22 (17) (2015) 13534–13545.
[3] P. Forster, T. Storelvmo, K. Armour, W. Collins, J.L. Dufresne, D. Frame, D.J. Lunt, T. Mauritsen, M.D. Palmer, M. Watanabe, M. Wild, H. Zhang, The Earth's energy budget, climate feedbacks, and climate sensitivity, in: Climate Change 2021: the Physical Science Basis. Contribution of Working Group I to the Sixth Assessment Report of the Intergovernmental Panel on Climate Change, Cambridge University Press, Cambridge, 2021.
[4] B.L. Bodirsky, A. Popp, H. Lotze-Campen, J.P. Dietrich, S. Rolinski, I. Weindl, C. Schmitz, C. Müller, M. Bonsch, F. Humpenöder, Reactive nitrogen requirements to feed the world in 2050 and potential to mitigate nitrogen pollution, Nat. Commun. 5 (2014), 3858.
[5] M. Miyahara, S.-W. Kim, S. Fushinobu, K. Takaki, T. Yamada, A. Watanabe, K. Miyauchi, G. Endo, T. Wakagi, H. Shoun, Potential of aerobic denitrification by *Pseudomonas stutzeri* TR2 to reduce nitrous oxide emissions from wastewater treatment plants, Appl. Environ. Microbiol. 76 (14) (2010) 4619–4625.
[6] Y.T. Li, Y.R. Wang, L. Fu, Y.Z. Gao, H.X. Zhao, W.Z. Zhou, Aerobic-heterotrophic nitrogen removal through nitrate reduction and ammonium assimilation by marine bacterium *Vibrio* sp. Y1-5, Bioresour. Technol. 230 (2017) 103–111.
[7] Y. Liu, G.M. Ai, L.L. Miao, Z.P. Liu, *Marinobacter strain* NNA5, a newly isolated and highly efficient aerobic denitrifier with zero N_2O emission, Bioresour. Technol. 206 (2016) 9–15.
[8] Y. Li, J. Ling, P. Chen, J. Chen, R. Dai, J. Liao, J. Yu, Y. Xu, *Pseudomonas mendocina* LYX: a novel aerobic bacterium with advantage of removing nitrate high effectively by assimilation and dissimilation simultaneously, Front. Environ. Sci. Eng. 15 (4) (2021), 57.
[9] F.D. Capua, F. Pirozzi, P.N.L. Lens, G. Esposito, Electron donors for autotrophic denitrification, Chem. Eng. J. 362 (2019) 922–937.
[10] Y.P. Zhang, G.B. Douglas, A.H. Kaksonen, L.L. Cui, Z.F. Ye, Microbial reduction of nitrate in the presence of zero-valent iron, Sci. Total Environ. 646 (2019) 1195–1203.
[11] S. Matassa, N. Boon, W. Verstraete, Resource recovery from used water: the manufacturing abilities of hydrogen-oxidizing bacteria, Water Res. 68 (2015) 467–478.
[12] X. Hu, P. Vandamme, N. Boon, Co-cultivation enhanced microbial protein production based on autotrophic nitrogen-fixing hydrogen-oxidizing bacteria, Chem. Eng. J. 429 (2022) 132535.
[13] L.J. Zhang, Y. Xie, L.Y. Ding, X.J. Qiao, H.C. Tao, Highly efficient ammonium removal through nitrogen assimilation by a hydrogen-oxidizing bacterium, *Ideonella* sp. TH17, Environ. Res. 191 (2020), 110059.
[14] P. Li, W. Xing, J. Zuo, L. Tang, Y.J. Wang, J. Lin, Hydrogenotrophic denitrification for tertiary nitrogen removal from municipal wastewater using membrane diffusion packed-bed bioreactor, Bioresour. Technol. 144 (2013) 452–459.
[15] U. Javourez, M. O'Donhue, L. Hamelin, Waste-to-nutrition: a review of current and emerging conversion pathways, Biotechnol. Adv. 53 (2021) 107857.
[16] S. Matassa, W. Verstraete, I. Pikaar, N. Boon, Autotrophic nitrogen assimilation and carbon capture for microbial protein production by a novel enrichment of hydrogen-oxidizing bacteria, Water Res. 101 (2016) 137–146.
[17] X. Hu, F.M. Kerckhof, J. Ghesquiere, K. Bernaerts, P. Boeckx, P. Clauwaert, N. Boon, Microbial protein out of thin air: fixation of nitrogen gas by an autotrophic hydrogen-oxidizing bacterial enrichment, Environ. Sci. Technol. 54 (6) (2020) 3609–3617.
[18] W. Zhang, F. Zhang, Y. Niu, Y.X. Li, Y. Jiang, Y.N. Bai, K. Dai, R.J. Zeng, Power to hydrogen-oxidizing bacteria: effect of current density on bacterial activity and community spectra, J. Clean. Prod. 263 (2020b) 121596.
[19] T.G. Volova, E.G. Kiselev, E.I. Shishatskaya, N.O. Zhila, A.N. Boyandin, D.A. Syrvacheva, O.N. Vinogradova, G.S. Kalacheva, A.D. Vasiliev, I.V. Peterson, Cell growth and accumulation of polyhydroxyalkanoates from CO_2 and H_2 of a hydrogen-oxidizing bacterium, *Cupriavidus eutrophus* B-10646, Bioresour. Technol. 146 (2013) 215–222.

[20] D.H. Huson, B. Buchfink, Fast and sensitive protein alignment using DIAMOND, Nat. Methods 12 (1) (2015) 59–63.
[21] APHA, Standard Methods for the Examination of Water and Wastewater, American Public Health Association, Washington, DC, 2012.
[22] B.E. Rittmann, P.L. Mccarty, Environmental Biotechnology: Principles and Applications, McGraw-Hill Companies, Inc., New York, NY, 2003.
[23] J. Dou, Y. Huang, H. Ren, Z. Li, Q. Cao, X. Liu, D. Li, Autotrophic, heterotrophic, and mixotrophic nitrogen assimilation for single-cell protein production by two hydrogen-oxidizing bacterial strains, Appl. Biochem. Biotechnol. 187 (1) (2019) 338–351.
[24] J. Yu, A. Dow, S. Pingali, The energy efficiency of carbon dioxide fixation by a hydrogen-oxidizing bacterium, Int. J. Hydrogen Energy 38 (21) (2013) 8683–8690.
[25] Y. Lu, J. Yu, Comparison analysis on the energy efficiencies and biomass yields in microbial CO_2 fixation, Process Biochem. 62 (2017) 151–160.
[26] S. Ebrahimi, T.H. Nguyen, D.J. Roberts, Effect of temperature & salt concentration on salt tolerant nitrate-perchlorate reducing bacteria: nitrate degradation kinetics, Water Res. 83 (2015) 345–353.
[27] S. Ghafari, M. Hasan, M.K. Aroua, Effect of carbon dioxide and bicarbonate as inorganic carbon sources on growth and adaptation of autohydrogenotrophic denitrifying bacteria, J. Hazard Mater. 162 (2–3) (2009) 1507–1513.
[28] S. Salehlakha, K.E. Shannon, S.L. Henderson, C. Goyer, J.T. Trevors, B.J. Zebarth, D.L. Burton, Effect of pH and temperature on denitrification gene expression and activity in *Pseudomonas mandelii*, Appl. Environ. Microbiol. 75 (12) (2009) 3903–3911.
[29] S. Zokaei-Kadijani, J. Safdari, M.A. Mousavian, A. Rashidi, Study of oxygen mass transfer coefficient and oxygen uptake rate in a stirred tank reactor for uranium ore bioleaching, Ann. Nucl. Energy 53 (2013) 280–287.
[30] D. Patureau, N. Bernet, J.P. Delgenes, R. Moletta, Effect of dissolved oxygen and carbon-nitrogen loads on denitrification by an aerobic consortium, Appl. Microbiol. Biotechnol. 54 (4) (2000) 535–542.
[31] J. Curko, M. Matosic, H.K. Jakopovic, I. Mijatovic, Nitrogen removal in submerged MBR with intermittent aeration, Desalination Water Treat. 24 (1–3) (2010) 7–19.
[32] Y.H. Zhang, F.H. Zhong, S.Q. Xia, X.J. Wang, Effect of initial nitrate concentrations and heavy metals on autohydrogenotrohic denitrification. 3rd International Conference on Bioinformatics and Biomedical Engineering, Institute of Electrical and Electronics Engineers, Beijing, China, 2009, pp. 5637–5640.
[33] X.J. Huang, C.G. Weisener, J.P. Ni, B.H. He, D.T. Xie, Z.L. Li, Nitrate assimilation, dissimilatory nitrate reduction to ammonium, and denitrification coexist in *Pseudomonas putida* Y-9 under aerobic conditions, Bioresour. Technol. 312 (2020), 123597.
[34] M.S. Zheng, D. He, T. Ma, Q. Chen, S.T. Liu, M. Ahmad, M.Y. Gui, J.R. Ni, Reducing NO and N_2O emission during aerobic denitrification by newly isolated *Pseudomonas stutzeri* PCN-1, Bioresour, Technol. 162 (2014) 80–88.
[35] Z. Shi, Y. Zhang, J.T. Zhou, M.X. Chen, X.J. Wang, Biological removal of nitrate and ammonium under aerobic atmosphere by *Paracoccus versutus* LYM, Bioresour, Technol. 148 (2013) 144–148.
[36] R.F. Jin, T.Q. Liu, G.F. Liu, J.T. Zhou, J.Y. Huang, A.J. Wang, Simultaneous heterotrophic nitrification and aerobic denitrification by the marine origin bacterium *Pseudomonas* sp. ADN-42, Appl. Biochem. Biotechnol. 175 (4) (2015) 2000–2011.
[37] Y.L. Sun, L. Feng, A. Li, X.N. Zhang, F. Ma, Ammonium assimilation: an important accessory during aerobic denitrification of *Pseudomonas stutzeri* T13, Bioresour. Technol. 234 (2017) 264–272.
[38] W. Zhang, Y. Niu, Y.X. Li, F. Zhang, R.J. Zeng, Enrichment of hydrogen-oxidizing bacteria with nitrate recovery as biofertilizers in the mixed culture, Bioresour. Technol. 313 (2020), 123645.
[39] S.Y. Lunt, M.V. Heiden, Aerobic glycolysis: meeting the metabolic requirements of cell proliferation, Annu. Rev. Cell Dev. Biol. 27 (1) (2011) 441–464.
[40] S.R. Kimball, L.S. Jefferson, Regulation of protein synthesis by branched-chain amino acids, Curr. Opin. Clin. Nutr. Metab. Care 4 (1) (2001) 39–43.
[41] M. Monirujjaman, A. Ferdouse, Metabolic and physiological roles of branched-chain amino acids, Adv. Mol. Biol. 2014 (2014) 364976.
[42] S. Ghafari, M. Hasan, M.K. Aroua, A kinetic study of autohydrogenotrophic denitrification at the optimum pH and sodium bicarbonate dose, Bioresour. Technol. 101 (7) (2010) 2236–2242.
[43] Y. Zhao, C. Feng, Q. Wang, Y. Yang, Z. Zhang, N. Sugiura, Nitrate removal from groundwater by cooperating heterotrophic with autotrophic denitrification in a biofilm-electrode reactor, J. Hazard Mater. 192 (3) (2011) 1033–1039.
[44] Q. Wang, C. Feng, Y. Zhao, C. Hao, Denitrification of nitrate contaminated groundwater with a fiber-based biofilm reactor, Bioresour. Technol. 99 (7) (2009) 2223–2227.
[45] K. Khosravi-Darani, Z.-B. Mokhtari, T. Amai, K. Tanaka, Microbial production of poly(hydroxybutyrate) from C-1 carbon sources, Appl. Microbiol. Biotechnol. 97 (4) (2013) 1407–1424.
[46] L.J. Zhang, H.C. Tao, Bioelectro-Fenton System for Environmental Pollutant Degradation, in: A.J. Wang, B. Liang, Z.L. Li, H.Y. Cheng (Eds.), Bioelectrochemistry Stimulated Environmental Remediation, Springer Nature Singapore Pte Ltd., Singapore, 2019, pp. 245–268.